DOI: 10.2478/sbeef-2022-0005

EVALUATION AND DEVELOPMENT OF A HYBRID RENEWABLE ENERGY SYSTEM FOR THE REMOTE TELECOMMUNICATION STATION OF BOUGAROUN, COLLO, ALGERIA

I. LOUAHEM M'SABAH, S. BENZAHIOUL, R. DJEGHADER, A. METATLA
LGMM Laboratory, Université 20 Août 1955-Skikda, PB N° 26 Route Elhadaik, Skikda 21000, Algeria
E-mail: i.louahemmsabah@univ-skikda.dz, s.benzahioul@univ-skikda.dz, r.djeghader@univ-skikda.dz, a.metatla@univ-skikda.dz

Abstract. ***Mobile telecommunication sites are an essential station in our technological life, used to allow the communication through mobiles and internet. Many telecommunication sites are installed in remote areas where the grid is not available. For this, hybrid renewable energy systems (HRES) are used to power the stations and integrate the remote areas with the world. This article aims to evaluate the performance of the existing HRES of the remote mobile telecommunication station of Bougaroun, Collo, Algeria - which consists of PV modules, batteries and diesel generator (DG)- and to develop it using a mathematical model to demonstrate the effect of deploying a wind turbine to supply more green energy, minimize the operation cost (fuel consumption and maintenance), and reduce the greenhouses emitted by the DG. Based on the wind data at the site location, the obtained results show a significant amount of output power that can be used to minimize the DG functionality.***

Keywords: Hybrid renewable energy system, PV, batteries, wind turbine, diesel generator, telecommunication; green energy.

1. INTRODUCTION

The field of information and technology (IT) has seen a continuous revolution in the last decades because of the huge demand and need of people to communicate through mobiles and to use the Internet in all fields. For this, researchers have developed new generations of telecommunication like (the fourth generation (4G), fifth generation (5G) and they are working to release the sixth generation (6G)). This technology is installed in the mobile telecommunication stations which are the base interface between the users and the network. As the number of subscribers increases, the consumption of the mobile station increases, and the continuity of the service becomes crucial.

One of the critical points that affect the stability of the service is the power supply, such that any shortage or loss of power supply due to a cut from the grid or a fully discharge of the batteries will shut down the station and disconnect the users from the world. Such events have many negative impacts on the life of people, like in economy where the business is affected, in research and development, and even in the social life where citizens emigrate from the rural areas to the cities (phenomena of rural exodus) and increase the pressure in the towns [1]. Therefore, the grid must be dependable and available to ensure the supply of energy to the stations.

The problem is that the reliability of the grid is out of control of the mobile station operators, and in the remote areas the grid is not even available due to the expansiveness of expanding the power system, and in mountains the access to some sites is difficult during the winter where the distribution lines can be failed down [2], and the road is blocked by the snow, so the DGs stops running after the fuel is fully consumed. So, to solve this problem, hybrid renewable energy sources are proposed to be used as a stand-alone or grid connected systems.

The term hybrid energy system refers to the use of different combinations of energy sources (PV, wind turbine (WT), battery, hydrogen tank (HT), DG) to produce power like PV/WT/batteries/DG system, PV/batteries/DG system, WT/Batteries system, batteries/DG system, etc.

Nowadays, most of the research focus on designing best hybrid renewable energy systems to exploit the free energy from the sun and the wind. The most two important points in the optimization are the system reliability and the overall cost. Below are brief summaries on some works related to HRES:

In order to reduce the cost of energy and enhance the performance of the telecommunication networks in the remote areas of the Maghreb, Hamza Siyoucef et al [3] simulated the energy production of a hybrid green energy system (PV-wind turbine) using MATLAB/Simulink to power a grid-connected mobile telecommunication Base Transceiver Station (BTS) [4], in three (3) different remote areas of the Maghreb (Ras El Oued, Cherb Errih,

and Ain Amara). The hybrid green energy system (HGRE) is implemented on HOMER software (Hybrid Optimization Model for Multiple Energy Resources) [5], to perform a techno-economic optimization (sizing) of the system based on the weather conditions of the regions. After simulating the PV and wind productions, DG emission and including the grid electricity price (€/kWh), HOMER obtained the PV-wind turbine system as the best solution based on the total net present cost (TNPC) and the levelized cost of energy (LCOE) [6].

The work presented in [7], investigates the use of PV-wind DC microgrid with a battery energy storage system to power the remote and isolated telecommunication towers instead of using the DGs. A techno-economic analysis is caried out with a multi-objective function which optimizes the COE, loss of power supply probability (LPSP) and the excess of energy (EE). The output power of the HRES is obtained from the mathematical models which took into consideration the de-rating factor and the maximum power point tracking (MPPT) factor. The multi-objective optimization is done based on a non-dominated sorting genetic algorithm II (NSGA II) [8], which ranks the population by non-dominant sorting and minimizes all the objectives simultaneously. Three (3) different scenarios are simulated:
- DC microgrid 100% dependable: the obtained solution is 106 PV panels of 250W, 9 kW wind turbine and 400 V, 306.63 Ah battery energy storage. The COE of the HRES is 0.218 $/kWh which is 35% lower than conventional DG system.
- DC microgrid with LPSP=0.038: the best size is 24 PV panels, 6.3 kW wind turbine, and 400 V, 247.1 Ah battery supplying 11.28 h back-up. The COE of the HRES is 0.179 $/kWh.
- DC microgrid with LPSP=0.2: the best solution is 47 PV panels, 30.8 kW wind turbine and 400 V, 189.3 Ah battery with 8.64 h back-up. In all scenarios, the SOC is kept greater than 50% to increase the lifespan of the batteries which are the most expensive components in HRES.

D.Abbes et al [9], introduced a new criterion to perfect the design of an HRES based on MATLAB, using a dynamic model and two different algorithms (fmincon function of MATLAB and a controlled elitist genetic algorithm) with single and multi-objective functions. The single aim is to minimize the embodied energy (EE) cost subjected to the constrains of minimum LPSP, and considering PV modules' installed area, wind turbine swept area and battery bank capacity (Ah) as decision variables. The multi-objective is to minimize both EE cost and LPSP using the second algorithm. The results of the mono-objective optimization supply a lower LPSP (4.881% <5%) but a higher total primary system EE compared to the multi-objective optimization (138189.14 MJ > 13749.3 MJ). Moreover, the analysis confirms that small wind turbines are more energy efficient than photovoltaic panels.

In [10], the authors proposed a multi-objective evolutionary algorithm based on decomposition (MOEA/D), using localized penalty-based boundary intersection (LPBI) to perfect a stand-alone and a grid connected HRES. In the first mode, the cost of system (Cs), fuel emissions (Fe) and the probability of unsatisfying the load demand (Pu) are to be minimized. For the grid-connected mode, the cost of system (Cs), fuel emissions (Fe) and the proportion of non-renewable energy (Pnre) are to be minimized. The best solution of each mode is obtained and compared to MOEA/D-PBI method, where the former method outperforms the latter one.

Motaz Amer et al [11], used particle swarm optimization (PSO) [12], to minimize the levelized cost of energy (LCE) of a PV/WT/battery system that is used to supply a house. The results of the optimization show that the minimum LCE is found to be 0.0030277 €/kW and the power generated from the wind turbine is 1.0185 kW, while the power generated from the PV module is 0.23153 kW taking into consideration that the load demand as an average was about 1 kW and the losses and the storage was taken as a percentage from the load.

Om Krishan and Sathans [13], used HOMER and MATLAB to compare the wind/battery, PV/battery, and wind/PV/battery systems with respect to the net present cost (NPC) and cost of energy (COE) to find the most economically practical option and to achieve 0% of unmet load. They found that the Wind/PV/battery system is the most economical configuration with a total NPC of 228,353 $ and COE of 0.288 $/kWh.

The authors [14], applied the genetic algorithm (GE) [15] to optimize a grid connected PV/wind/battery hybrid system using a novel energy filter algorithm to regulate the power injected into the grid. The aim is to minimize the total cost of the hybrid system under the constraints of loss of power supply probability, full use of complementary characteristics, fluctuations in the power injected into the grid, and the battery state of charge (SOC). Compared to the case of an optimization without an energy filter and with an energy filter, the proposed method with the developed energy filter algorithm gives the cost-effective combination of the system components, while satisfying all the required constraints.

1.1 Related work

Our work analyses the performance of the actual HRES of Bougaroun, Collo, Skikda, Algeria, mobile telecommunication site, that consists of PV modules, batteries and DG, and demonstrates the effect of integrating a small wind turbine based on the wind speed in the site location, in order to minimize the supplying rate of the DG which emits the CO2 in the atmosphere, and reduce the discharge capacity of the batteries to extend their life time and hence reducing the system total cost affected by the expensive prices of the batteries (the reduction of the batteries discharge means a decrease in the number of a battery replacement during the project life).

2. DESCRIPTION OF THE SITE AND ITS DATA

The site of Bougaroun is a terminal 3G (third generation) mobile telecommunication station, found in a remote area where the grid is unavailable. For this, 33 PV modules are used as the main power source during the sunshine hours, 96 lead acid batteries and a DG which supplies the load and charges the batteries when they reach the selected depth of discharge (DOD). The ratings of the energy system are as follow:

• PV module: 30.13V, 8.30A, 250 W (BYD250P6C-30) (Figure 1).
• Battery: 2V, 650 Ah (AGISSON TCB-650A1) (Figure 2).
• DG: 17 KVA/ 14 kW (Figure 3).

Figure 1. The 250W photovoltaic panels.

Figure 2. The lead acid batteries.

Figure 3. The 14kW diesel generator.

The load consists of a 2G (second generation)/3G BTS, Radio Transmission Network (RTN 950), and a DC air conditioner, in addition to the sensors and monitoring equipment which do not consume much energy.
The ratings of the load are:

• BTS3900: -48V/ 78A (Figure 4).
• RTN 950: -48V/14.3A (Figure 5).
• DC air conditioner: -48V/20A (Figure 6).

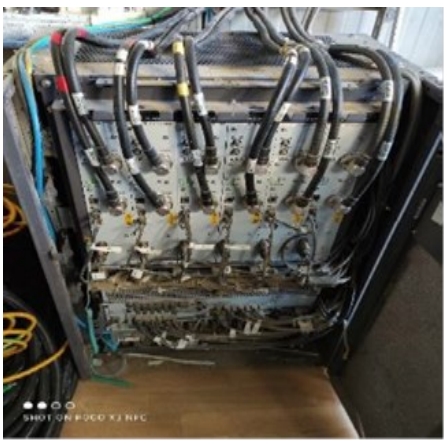

Figure 4. The BTS 3900.

Figure 5. The RTN 950.

Figure 6. The DC air conditioner.

The data of the load consumption, PV output power, batteries charge / discharge capacities, and the DG power supply are exported from the Energy Control Centre of the system which can store the data of one month as maximum.

2.1 Load profile

Figure 7 is the daily DC load energy consumption for the period between June 1st, 2021, and January 31st, 2022. The minimum energy consumption is 25.02 kWh on December 3rd (some loads were disconnected for the swap and upgrade), the maximum value reached 81.78 kWh on August 10th (meets an official holiday related to an Islamic event "Ashura" where people call each other, so the energy consumption increases) and the average value of the energy consumption is 61.16 kWh/day. The total energy consumed in this period is 14985.32 kWh.

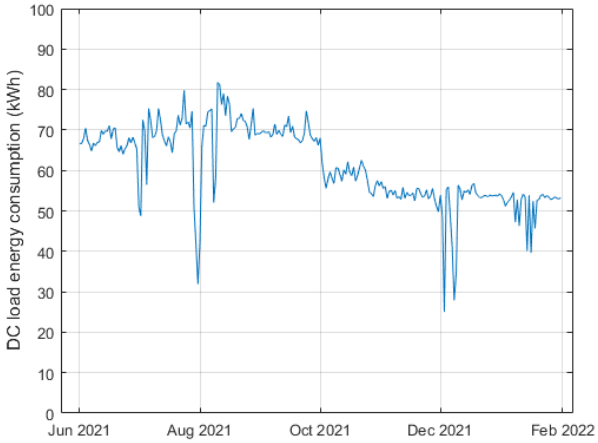

Figure 7. DC load energy consumption of the site.

2.2 PV supply

Figure 8 shows the energy supplied by the PV modules during the same period, which is directly proportional to the solar irradiance. The peak value of the supplied energy is 57.84 kWh on June 8th, 2021, while the lowest energy supplied is 0.103 kWh recorded on January 10th, 2022 (cloudy day). The average value of the solar system energy production is 33.02 kWh/day (54.2% of the load average consumption). The total energy produced by the solar system is 8091.334kWh.

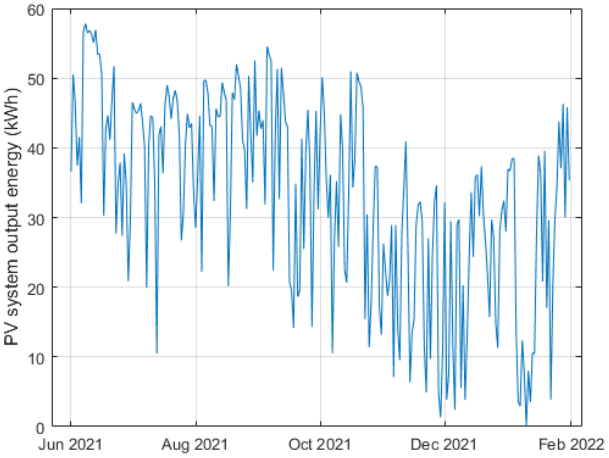

Figure 8. PV system output energy.

2.3 Batteries discharge capacity

The 2600 Ah batteries system start discharging when the energy produced by the PV system is less than the load demand (Figure 9). The maximum discharge capacity reached 48.94 kWh on June 29th, 2021 (the storage system discharged during the night and during most of the sunshine hours, because the output energy of the PV system was less than the load demand. So, the source of supply was PV and battery), the minimum value is 5.75 kWh recorded on August 1st, 2021 (the batteries were discharging before this day and continued to discharge

from August 1st at 00:00AM to 7:00AM until the solar system started to generate the energy which was not enough to charge the batteries quickly. Once the PV output energy became less than the load demand, the batteries discharged again and reached the smallest DOD (60%). So, the DG ran for the remaining hours and the batteries stopped supplying the load. That is why the discharge capacity was minor compared to the other days). The average discharge capacity is 33.63 kWh/day (54.9% of the load average consumption), and the total energy supplied by the batteries is 8240.981 kWh.

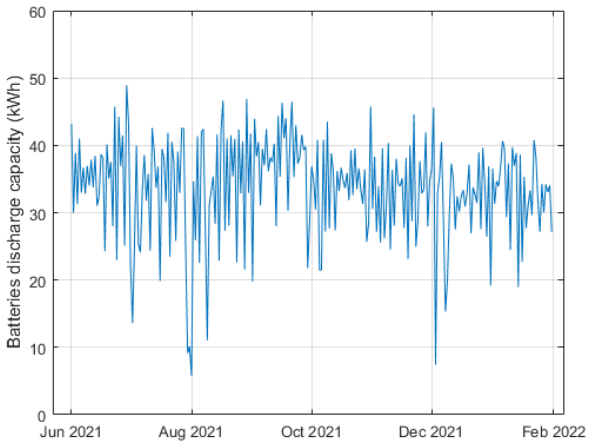

Figure 9. The storage system output energy.

2.4 DG power supply

The DG is set to start when the batteries reach the selected depth of discharge (DOD). When it runs, it supplies the energy to the batteries and the load. In case the batteries are fully charged, or the PV output energy is greater than the load demand, the DG stops. Figure 10 shows the energy produced by the DG for each day between June 1st, 2021, and January 31st, 2022. The highest value of the generated energy reached 99.07 kWh on January 10th where the PV output energy was close to zero (in the previous day the total PV output energy was 7.55 kWh, so the batteries discharged all day. When it came to January 10th, the batteries reached the DOD, and the DG ran for 11 hours). In many days when the batteries did not reach the DOD, the DG did not start. The average energy produced is 34.79 kWh/day (56.8% of the load average consumption) and the total energy supplied by the DG is 8525.441kWh.

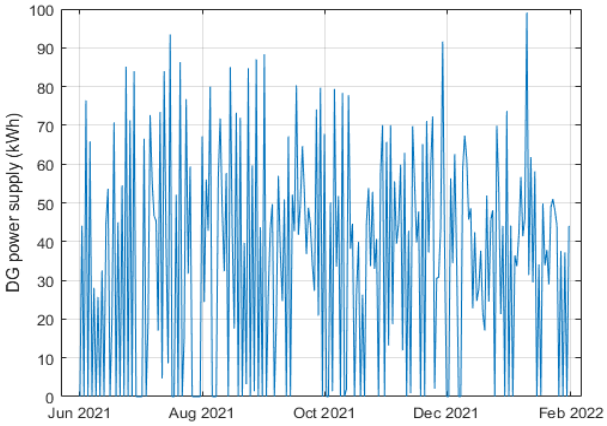

Figure 10. DG generated energy.

2.5 Wind potential

The data of the wind speed in the cap of Bougaroun, Collo, Skikda, Algeria is extracted from NASA prediction of worldwide energy resources website [16]. The data are recorded at the height of 50m above the ground, for the duration between March 1st, 2021, and March 1st, 2022.

From Figure 11 the maximum daily speed is 14.53 m/s on December 10th, 2021, while the minimum value reached 1.71 m/s on January 1st, 2022. The average daily wind speed for this period is 5.01 m/s. These data will be used in the next sections to calculate the output energy of the proposed wind turbine using a mathematical model.

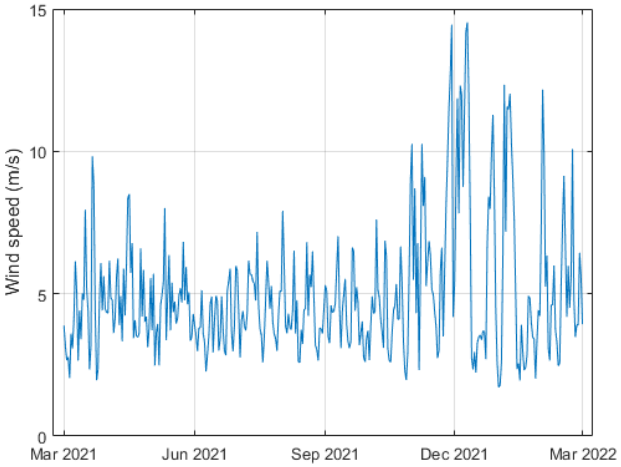

Figure 11. Daily wind speed.

3. MODELLING OF THE HRES COMPONENTS

Mathematical models are used to:

- Calculate the output energy of the PV modules and wind turbines based on the meteorological data.
- Find the state of charge of the batteries (SOC) for each time step.
- Calculate the fuel consumption of the DG based on its generated energy.

The power generated by the DG depends on the load profile, the power produced by the renewable energy components (PV and wind turbine), the SOC of the batteries, and the management strategy of the system.

3.1 PV model

The output power of the PV module is equal to the open circuit voltage times short-circuit current multiplied by the fill factor (FF) [17].

$$P_{pv}(t) = v_{oc}(t) \,.\, i_{sc}(t) \,.\, FF \qquad (1)$$

Where:
v_{oc} - open-circuit voltage (V).
i_{oc} - short-circuit current (A).
FF - Fill Factor.

These two parameters (v_{oc}, i_{oc}) are dependent to the solar radiation and ambient temperature as shown in the following equations [18]:

$$i_{SC}(G,T) = \frac{G}{G_{STC}}\left[i_{SC,STC} + \mu_{i_{SC}}(T - T_{STC})\right] \qquad (2)$$

Where:
G - solar irradiance (W/m^2).
T - PV module temperature (C°).
G_{STC} - solar irradiance at standard test conditions.
T_{STC} - PV module temperature at standard test conditions (C°).
$\mu_{i_{SC}}$ - thermal coefficient of the short-circuit current (A/C°).

$$v_{oc}(G,T) = v_{oc,STC} + \frac{N_s K T n}{q}\ln(G) + \mu_{v_{OC}}(T - T_{STC}) \qquad (3)$$

Where:
$v_{oc,STC}$ - open-circuit voltage at standard test conditions.
N_S - number of the series-connected cells in a PV module.
K - Boltzmann constant (1.381×10^{-23} J/K).
n - diode ideality factor.
q - electronic charge (-1.602×10^{-19} C).
$\mu_{v_{OC}}$ - thermal coefficient of the open-circuit voltage (V/C°).

3.2 Wind turbine model

The output power of the wind turbine depends on the wind speed at the hub height and the speed characteristics of the turbine [19].

$$P_{wind} = \begin{cases} P_R \dfrac{v - v_c}{v_r - v_c}, & \text{for } v_c \le v \le v_r \\ P_R, & \text{for } v_r \le v \le v_F \\ 0, & \text{for } v < v_c \text{ or } v > v_F \end{cases} \qquad (4)$$

Where:
P_R - rated power of the wind turbine.
v - wind speed.
v_r - rated wind speed.
v_c - cut-in wind speed.
v_F - cut-off wind speed.

3.3 Battery model

The state of charge of a battery can be modelled during the charge mode and discharge mode. In this model the SOC is expressed in (Wh) [20].
• During charging process:

$$C_{batt}(t) = C_{batt}(t-1) + (P_{RE}(t) - \frac{P_{load}(t)}{\eta_{inv}})\eta_{ch}\Delta t \qquad (5)$$

Where:
C_{batt} - battery capacity.
P_{RE} - Power produced by the renewable energy components.
P_{load} - power demand of the load.
η_{ch} - charging efficiency.
η_{inv} - inverter efficiency.
Δt - time step.

• During discharge process:

$$C_{batt}(t) = C_{batt}(t-1) + (P_{RE}(t) - \frac{P_{load}(t)}{\eta_{inv}})\frac{\Delta t}{\eta_{disch}} \qquad (6)$$

3.4 DG fuel consumption model

The fuel consumption of one hour is calculated using the following equation [21]:

$$F(t) = 0.246 \cdot P_{DG}(t) + 0.08415 \cdot P_R \qquad (7)$$

Where:
$F(t)$ - Fuel consumption in (L/h).
P_{DG} - power generated by the DG.
P_R - rated power of the DG.

4. RESULTS AND DISCUSSIONS

In this section the wind potential presented in 2.5 is used to calculate the energy generated from a small wind turbine, then it is compared with the real energy generated by the actual system during the period of June 1st and

January 31st, 2022, as shown in section 2.
The characteristics of the wind turbine are presented in Table 1.

Table 1. The characteristics of the wind turbine

Parameter	Value
Rated power	3 kW
Cut in speed	2.5 m/s
Cut out speed	None- continuous operation
Rated speed	12 m/s
Survival wind speed	70 /s

4.1 Wind turbine energy

Using the model of 3.2, the output energy of the selected wind turbine is shown in the next graph (Figure 12). The maximum energy production is recorded on August 2nd as 41 kWh, which represents 62.23% of the load demand of that day. On June 9th, 10th, 22nd, July 9th, 19th, and September 17th, there is no output energy because the wind speed is less than the cut-in speed of the turbine. The average energy generated is 13.86 kWh/day, and the total supplied energy is 1691.1 kWh.

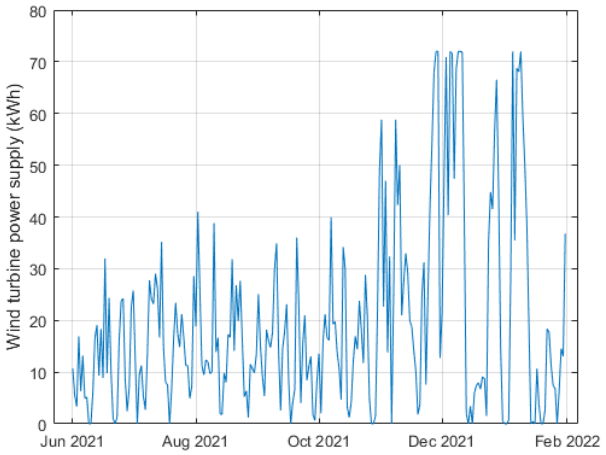

Figure 12. Wind turbine output energy.

Figure 13 shows the rate of supply of the PV/batteries/DG system as a percentage of the load energy consumption for each month. The PV system rate of supply is decreasing going from June to January as the solar radiation decreases, while the DG supply rate is increasing significantly as expected from 39.65% in June to 67.17% in January with a peak of 76.42% in November because of the decrease in the solar system output. So, the DG runs more to supply the load and charge the batteries. Unfortunately, this behaviour of the system increases the cost of operation (fuel consumption and maintenance) and emits more CO2 in the environment while the world is fighting against greenhouse gases.

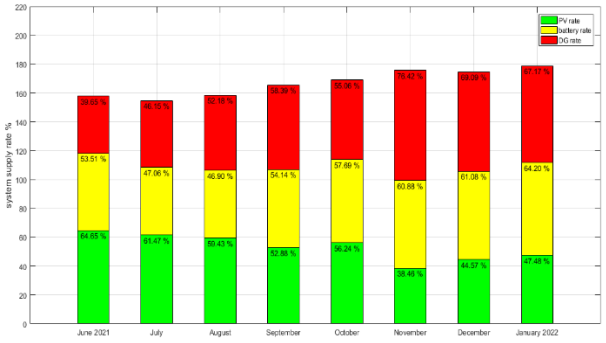

Figure 13. HRES rate of supply.

To reduce the cost of operation, the emission of CO2 and contribute to saving the environment, it is necessary to integrate the proposed wind turbine in the system. Figure 14 represents the rate of supply of the wind turbine as a percentage of the load consumption. During the summer, the wind turbine can produce around 20% of the load consumption, then in the Autumn and Winter the rate increases up to 66.38% in December which is a significant potential that must be exploited for the reduction of the DG supply and the generation of green energy.

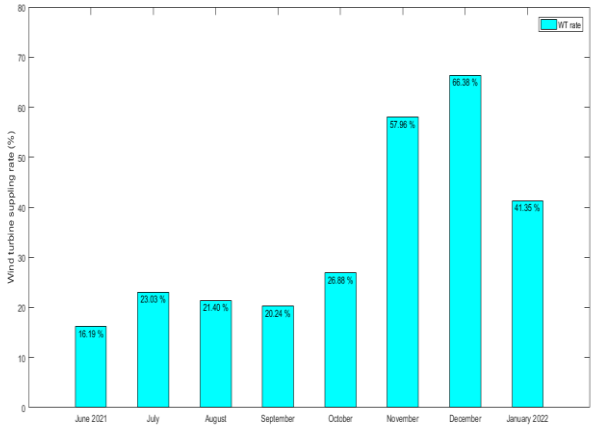

Figure 14. Wind turbine rate of supply.

5. CONCLUSION

This paper evaluated the operation of the existing HRES of Bougaroun mobile telecommunication station which shows that the PV output energy is the highest rate of supply in June, while the DG power supply is the lowest rate. In the next months, the equation reversed where the solar system rate decreased as a function of the solar radiation, and the DG supply rate increased to balance the energy flow. This increase in the DG operation, led us to study the deployment of a wind turbine to supply more free and green energy, and to limit the functionality of the conventional generator. The results show that in these months of Autumn and Winter, the wind turbine can supply a considerable amount of power.

These results encourage us to continue extracting the data each month until June 2022 in order to perform a techno-

economic optimization (sizing) of a PV/WT/battery/DG system and implement an optimal management strategy in order to increase the reliability, reduce the system total cost which is a critical point in HRES, decease the cost of operation and limit the CO2 emissions of the DG.

6. REFERENCES

[1] Cook, P. Infrastructure rural electrification and development. Energy for Sustainable Development 2011; 15(3): 304-313.

[2] Mitchell, J.W. Power line failures and catastrophic wildfires under extreme weather conditions. Engineering Failure Analysis 2013; 35: 726-735.

[3] Siyoucef, H., Benameur, A., Djilani Kobibi, Y.I., Ghouali, S., Merabet, B. and Motahhir, S. Performance Analysis and Techno-Economic Optimization of Green Energy Systems for Remote Areas in the Maghreb. Technology and Economics of Smart Grids and Sustainable Energy 2021; 6(12):12.

[4] Widjonarko, Avian, C., Budi Utomo, S., Setiawan, A. and Rudiyanto, B. A control strategy for hybrid energy source in backbone base transceiver station using artificial neural network: a case study of Penajam, Indonesia, International Journal of Energy and Environmental Engineering 2020; 11: 405-416.

[5] https://www.homerenergy.com/.

[6] Rehman, S., Rahman, H., Wang, S., Büker, M.S., Alhems, L.M. and AL Garni, H.Z. Optimal Design and Model Predictive Control of Standalone HRES: A Real Case Study for Residential Demand Side Management. IEEE Access 2020; 8: 29767-29814.

[7] Kaur, R., Krishnasamy, V. and Kandasamy, N.K. Optimal sizing of wind–PV-based DC microgrid for telecom power supply in remote areas. The institution of engineering and technology renewable power generation journal 2018; 10(7): 859-866.

[8] Deb, K., Pratap, A., Agarwal, S. and Meyarivan, T. A fast and elitist multi-objective genetic algorithm: NSGA- II. IEEE Transaction on Evolutionary Computation 2002; 6(2): 182–197.

[9] Abbes, D., Martinez, A. and Champenois, G. Eco-design optimization of an autonomous hybrid wind–photovoltaic system with battery storage. IET Renewable Power Generation 2012; 6(5): 358–371.

[10] Mengjun, M., Rui, W., Yabing, Z. and Tao, Z. Multi-Objective Optimization of Hybrid Renewable Energy System Using an Enhanced Multi-Objective Evolutionary Algorithm. Energies 2017; 10(5): 674.

[11] Motaz, A., Namaane, A. and M'Sirdi, N.K. Optimization of HRES using PSO for cost reduction. The Mediterranean Green Energy Forum, MGEF-13. Energy Procedia 2013; 42: 318 – 327.

[12] Kashani, A.R., Chiong, R., Mirjalili, S. and Gandom, A.H. Particle Swarm Optimization Variants for Solving Geotechnical Problems: Review and Comparative Analysis. Archives of Computational Methods in Engineering 2020; 28: 1871–1927.

[13] Krishan, O. and Sathans, S. Techno-economic analysis of a hybrid renewable energy system for an energy poor rural community. Journal of Energy Storage 2019; 23: 305–319.

[14] Aeidapu, M. and Kanwarjit, S.S. A genetic algorithm based improved optimal sizing strategy for solar-wind-battery hybrid system using energy filter algorithm. Frontiers in Energy 2017; 14: 139–151.

[15] Katoch, S., Chauhan, S.S. and Kumar, V. A review on genetic algorithm: past, present, and future. Multimedia Tools and Applications 2020; 80: 8091–8126.

[16] NASA Prediction of Worldwide Energy Resources. https://power.larc.nasa.gov/data-access-viewer/

[17] Bilal, B.O., Sambou, V., Ndiaye, B.A. and Kébé, C.M.F. Multi-objective Design of PV-Wind-Batteries Hybrid Systems by Minimizing the Annualized Cost System and the Loss of Power Supply Probability (LPSP). IEEE International Conference on Industrial Technology (ICIT), Cape Town, South Africa, 2013: 861–868.

[18] Haider, I. and Nader, A. Variations of PV module parameters with irradiance and temperature. 9th International Conference on Sustainability in Energy and Buildings, SEB-17, Chania, Crete, Greece, 2017: 276-285.

[19] Bhandari, B., Lee, K.T, Lee, G.Y., Cho, Y.M, and Ahn, S.H. Optimization of Hybrid Renewable Energy Power Systems: A Review. International journal of precision engineering and manufacturing-green technology 2015; 2(1): 99-112.

[20] GABOUR, A. Optimization et Commande d'un système énergétique multi source. Department of mechanical engineering, university of 20 Août 1955, Skikda, Algeria. Published PhD thesis 2019.

[21] Suryoatmojo, H., Hiyama, T., a Elbaset, A. and Ashari, M. Optimal Design of Wind-PV-Diesel-Battery System using Genetic Algorithm. IEEJ Transactions on Power and Energy 2009; 129(3): 413-420.